

DEVELOPMENT OF ADAPTIVE SEED-SEPARATION TRIER FOR SMALL-SEEDED CROPS

Elchyn ALIIEV¹ Krystyna LUPKO¹ Oleksandr KOBETS²

Abstract: *The STAR-CCM+ software package was used to create a model of the process of separating seed material from small-seeded crops on a cylindrical cellular trier. By taking into account the physic-mechanical properties of mustard seeds and the given initial and boundary conditions of the trier, a visualization of the separation process was obtained, which depended on several factors, including the number of seeds and impurities in the seed mixture, the rotation frequency of the trier cylinder, and the diameter of the trier cylinder. The numerical simulation of the process at a variable rotation frequency resulted in obtaining a relationship between the number of seeds and impurities, the relative content of impurity elements in the seed mixture in the tray, and the conditional performance of the separator, depending on the duration of cylinder rotation counterclockwise and clockwise. Based on the obtained dependencies of the numerical modeling and the results of improvement of the TracTrac software package, a laboratory sample of an adaptive cylindrical cell trier was developed. This trier allows in real time, based on the received video image, to determine the trajectory of the seed flight and to control the position of the tray and the rotation frequency of the cylinder using Arduino UNO.*

Key words: *separation, seed, length, trier, modeling, parameters, adaptive.*

1. Introduction

The separation process is crucial in the seed processing of small-seeded crops and is utilized at various stages [9]. It relies on

technical and technological principles that distinguish individual seed components based on their physical and mechanical properties. These properties comprise shape, size, weight, specific gravity,

¹ Institute of Oilseed Crops of the National Academy of Agrarian Sciences of Ukraine, Dnipro State Agrarian and Economic University, Ukraine;

² Dnipro State Agrarian and Economic University, Ukraine;
Correspondence: Elchyn Aliiev; email: aliev@meta.ua.

surface condition, and other factors that differentiate the primary seed from impurities [7], [11], [17]. The quality of the seed material and its stability during storage depends on the quality of seed material separation, and the quality of separation in turn depends on the correct selection of seed cleaning equipment [2].

Cylindrical triers are seed cleaning machines designed for separating seeds of different lengths. The trier comprises a cylinder with an internal cellular surface and a collection bin mounted on the axial support of the cylinder. Its functioning is rooted in the rotation of the cylinder, which causes seeds with distinct geometric dimensions to drop into the cellules [27]. Seeds that are long and have low resistance while at rest are carried in the direction of the cylinder's rotation and fall out of the cellules at a specific angle. On the other hand, short seeds with high resistance at rest fall out of the cellules at a different angle. All the seeds must drop out of the cellules, which depends on the equipment's structural parameters, including the cylinder's rotation frequency and diameter. To increase the efficiency of the process of separating seeds by their length, we have developed the design of an adaptive seed-separation trier [1], which is additionally equipped with a stepper motor, the shaft of which is fixed to the tray, a stepper motor-damper, which is installed in the bin-dozer, a camera, a lens of which is directed to the middle of the cylinder with the cellules and the control unit installed on the front part of the tray, which is connected to the gear motor, stepper motor, stepper motor-valve and camera with the help of electrical wires (Figure 1). To ensure that the designed trier is adaptable, it is crucial to identify the patterns of variation in the

process's technological parameters for separating seed material from small-seeded crops. This can be accomplished by utilizing numerical modeling to evaluate the impact of the trier's structural and mode parameters. The numerical modeling process can be carried out using various approaches. Currently, their classification includes the following methods [15]: empirical; analysis of the structure of material flows using the particle residence time distribution function; mechanics of continuous environments; entropy-informational; statistical. The following typical mathematical models of the material flow structure have become widespread among researchers: models of ideal extrusion and ideal mixing, diffusion and combined models [6], [16]. The strategy of complex system analysis of a physical and mechanical system involves a qualitative analysis at the initial stage. At the same time, two levels of the hierarchy of physic-mechanical effects and phenomena are distinguished for the separation process: a set of physic-mechanical phenomena in an elementary volume (micro level); a set of physical and mechanical phenomena in the volume of the entire device (macro level).

Numerous research studies have been conducted to address similar concerns [5], [8], [10], [19], [22]. These studies employed CFD and DEM to simulate experimental data pertaining to the dispersion of solid particles in a given volume. In some investigations [10], the STAR-CCM+ software was utilized to establish conditions for increasing the removal efficiency of small particles from an existing cyclone. In another study [22], researchers attempted to visualize the flow behavior of particles in various pipe geometries using the finite element method.

In the finite element method used for modeling the process, initial positions, particle velocities, and flow are established. Based on these initial data and given physical laws of contact interaction, forces acting on each particle in each time interval are calculated. The resulting power is then determined for each particle, and the Cauchy problem is

solved for a chosen time interval, with the outcome serving as initial data for the subsequent step [3]. Drawing on our own expertise [3, 4], [23-25] and the research mentioned earlier, we propose using the finite element method to address the set problems, which we implemented during modeling in the STAR-CCM+ software package.

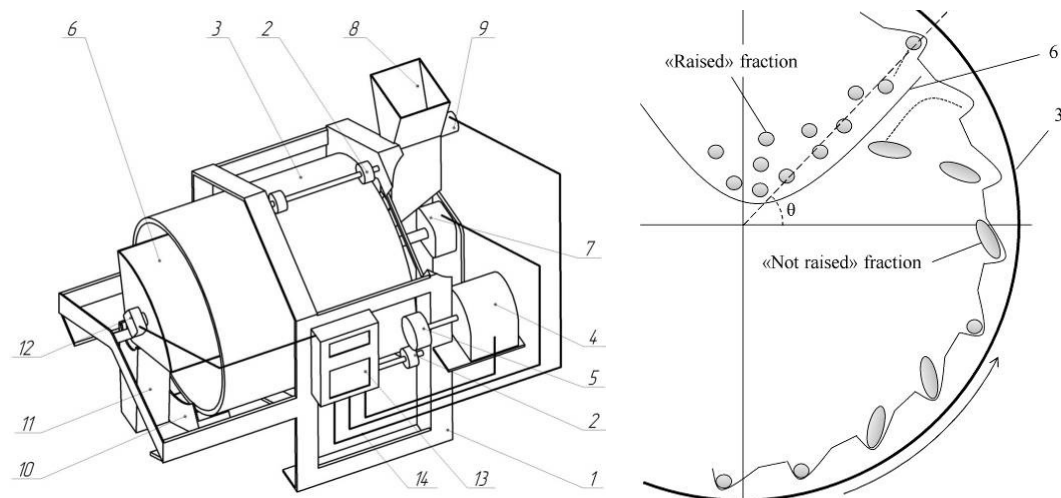


Fig. 1. *Structural and technological scheme of the adaptive seed-separation trier:*
 1 – frame; 2 – supporting rollers; 3 – cylinder with cellules; 4 – gear motor; 5 – drive roller; 6 – tray; 7 – stepper motor; 8 – bin-dozer; 9 – step motor-valve; 10 – collector of larger seeds; 11 – collector of smaller seeds; 12 – camera; 13 – control unit; 14 – electrical wires

2. Materials and Methods

Physical models such as the $k-\epsilon$ model of turbulence for separated flow, gravity field, Van der Waals real gas model, discrete element model, and multiphase interaction model were selected for numerical simulation [5], [21], [26]. The discrete element method is founded on the laws of impulse and moment of impulse conservation for Lagrangian models of a multiphase medium. However, to construct a physical-mathematical model, it is necessary to

assume that the seeds are identical ellipsoids with a particular density and effective diameter.

Mustard seeds were used as the seed model, with the following physical and mechanical properties: Poisson's ratio of 0.5, Young's modulus of 0.2 MPa, density of 700 kg/m^3 , coefficient of rest friction of 0.8, normal recovery factor of 0.5, tangent coefficient of recovery of 0.5, and coefficient of rolling resistance of 0.3. The model for the mustard seed is a sphere (Figure 2). At the same time, the effective seed diameter complies with a normal

distribution and is characterized by the probability density (Figure 3):

$$f(d_g, \bar{d}_g, \sigma_g) = \frac{1}{\sigma_g \sqrt{2\pi}} \exp\left(-\frac{(d_g - \bar{d}_g)^2}{2\sigma_g^2}\right) \quad (1)$$

where: $\bar{d}_g = 0,002$ m; $\sigma_g = 0,001$ m.

At the same time, the seeds can have an effective diameter that is in the range $d_g \in [d_{gmin}; d_{gmax}]$, where $d_{gmin} = 0.001$ m; $d_{gmax} = 0.003$ m. The seed mixture was comprised of two components: the seeds of the main crop and impurity elements.

The physical and mechanical properties of the impurity elements in the seed mixture were assumed to be: Poisson's ratio of 0.5, Young's modulus of 0.2 MPa, density of 700 kg/m³, coefficient of rest friction of 0.8,

normal recovery factor of 0.5, tangent coefficient of recovery of 0.5, and coefficient of rolling resistance of 0.3. The model of impurity elements is shown in Figure 1b. At the same time, the effective diameter of impurity elements complies with a normal distribution and is characterized by the probability density (Figure 3):

$$f(d_i, \bar{d}_i, \sigma_i) = \frac{1}{\sigma_i \sqrt{2\pi}} \exp\left(-\frac{(d_i - \bar{d}_i)^2}{2\sigma_i^2}\right) \quad (2)$$

where: $\bar{d}_i = 0.003$ m; $\sigma_i = 0.001$ m.

At the same time, the seeds can have an effective diameter that is in the range $d_i \in [d_{imin}; d_{imax}]$, where $d_{imin} = 0.002$ m; $d_{imax} = 0.004$ m.

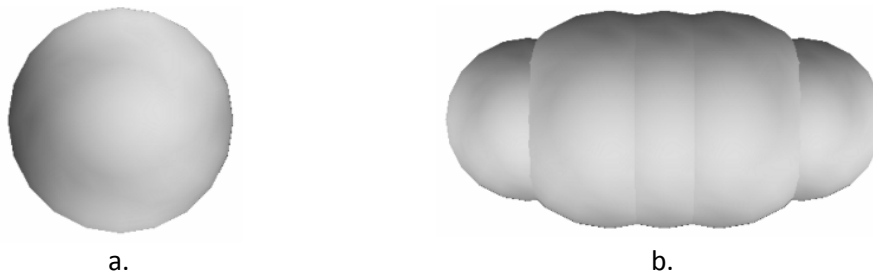


Fig. 2. Models of seeds (a.) and impurity elements (b.)

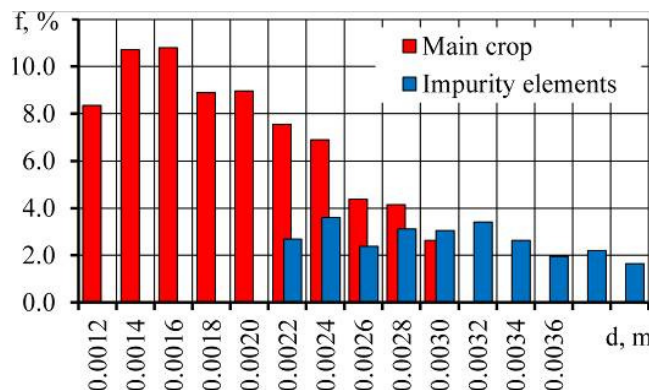


Fig. 3. Distribution of the number of seeds of the main crop and impurity elements according to their effective diameter

The environmental parameters for the simulation were set as follows: the medium was air with a dynamic viscosity of $1.85508 \cdot 10^{-5}$ Pa·s and a turbulent Prandtl number of 0.9; the free-fall acceleration was 9.8 m/s^2 ; the temperature was set at 293 K, and the pressure was set to 101325 Pa.

According to some studies [20], the geometric dimensions of the cellules are taken as in Figure 4.

The model's grid is the place where the process of separation of the seed material takes place. It is limited by a surface, thanks to which the seed material will not cross it. The model's grid is presented in the form of polyhedral cellules of different sizes. Therefore, the size of the cellules affects the quality of the calculation (the smaller the size of cellules, the higher the

quality of calculation) and, accordingly, acts the calculation time. As a result of preliminary modulation, it was established that the rational size of the cellules of the simulation grid is 0.0012 m (Figure 5).

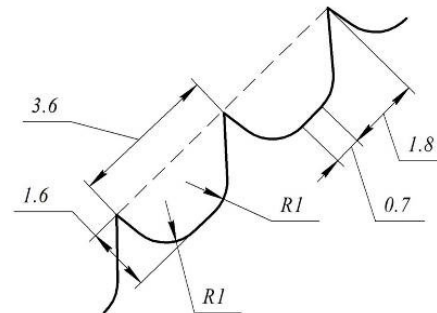


Fig. 4. Geometric dimensions of the cellules of the selection-seed cylindrical trier (in mm)

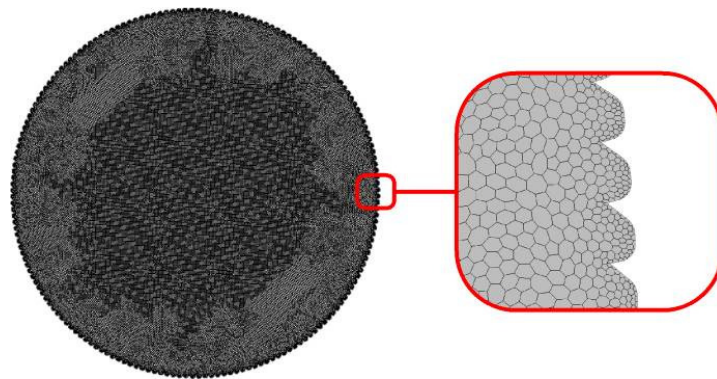


Fig. 5. Grid of the numerical simulation model in the STAR-CCM+ software package

The process of separating seed material of small-seeded crops by length in the standard mode (with the trier cylinder rotating in one direction) was simulated using numerical methods. The simulation began by presenting the calculation scheme for the cylindrical seed-separation trier (Figure 6). Figure 6 shows two flat images of a seed-separation trier cylinder with seed material in a cross-section in the

xOy coordinate system: on the left side, the cylinder is at rest, and on the right side, during clockwise rotation for 20 seconds.

The diameter of cylinder D is constant. The essential criteria were the determination of the maximum θ_{\max} and minimum θ_{\min} angles of rotation at the moments of the emergence of the first component of the seed material and the

last one. The number of seeds N_0 in the interval between θ_{max} and θ_{min} is an indirect indicator of the performance of

the trier because, during the rotation of the cylinder, the seed material rises along the movement path.

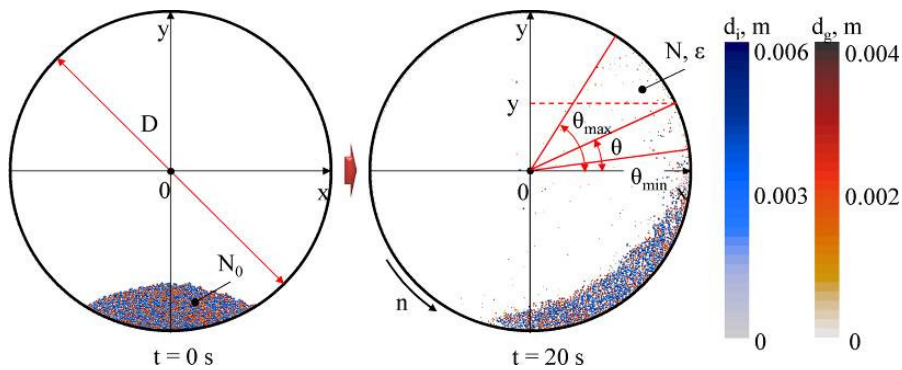


Fig. 6. Scheme for calculating a cylindrical trier with cellules for numerical modeling using the STAR-CCM+ software package

During the rotation of the trier cylinder, long impurity elements fall out of the cellules without reaching the region of θ_{min} and θ_{max} , but there is a concept of randomness in which, under random conditions, the impurity elements reach the region between θ_{min} and θ_{max} . The quality of the seed separation process depends on the number of impurity elements that have entered the gap between θ_{min} and θ_{max} .

The numerical modeling factors included the diameter (D) of the seed-separation trier cylinder, its rotation frequency (n), and the number of seeds in the seed mixture (N_0) at the initial time. The levels of variation for these factors are presented in Table 1. The full factorial experiment was conducted with a total of 125 experiments (5^3).

Table 1

Levels of variation by numerical modeling factors

Level	Factor		
	Trier cylinder diameter D [m]	Trier cylinder rotation frequency n [rpm]	The number of seeds and impurity elements in the see d mixture N_0 [pcs]
	(x_1)	(x_2)	(x_3)
-1.0	0.2	30.0	1000
-0.5	0.3	37.5	2000
0	0.4	45.0	3000
+0.5	0.5	52.5	4000
+1.0	0.6	60.0	5000

At the moment the seed exits the cellules, the value of the angle θ of the polar coordinate system and the

coordinate y of the Cartesian coordinate system were recorded in Figure 6. An example of the height distribution of the

placement of the components of the seed mixture depending on their effective diameter is shown in Figure 7.

The lower and upper bounds of θ , which represents the angle of seed exit from the cellules, were determined.

The performance criterion was defined as the number of components in the seed mixture, denoted by N , that fell within the rotation angles of the seed-separation trier cylinder, ranging from the minimum value θ_{\min} to the maximum value θ_{\max} .

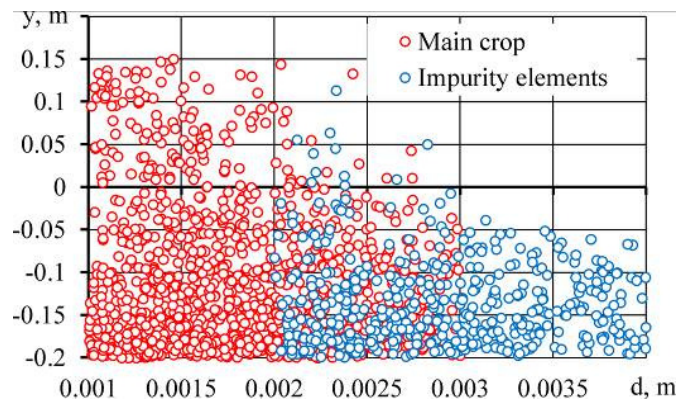


Fig. 7. Height distribution of the placement of the seed mixture components depending on their effective diameter d at $D = 0.4$ m, $n = 45$ rpm, $N_0 = 2000$ pcs

The relative content of impurity elements ε within the minimum θ_{\min} and maximum θ_{\max} angles of rotation of the seed-separation trier cylinder was adopted as a criterion for evaluating the quality of the separation process.

The study of the effect of changing the direction of rotation of the trier cylinder on the quality of the separation process was carried out as follows. The calculation scheme of the cylindrical cellules trier is presented in Figure 8. The difference between the new calculation scheme and the scheme in Figure 6 is the presence of a tray for collecting seeds, which is inclined at an angle θ_1 between the horizontal line and the wall of the tray. As a result of the movement of the component of the seed mixture, which is in the cell, the tray is filled with seeds and impurity elements. The resulting mixture is characterized by the number of seeds and impurity

elements in the seed mixture of the tray N_1 and the relative content of impurity elements ε_1 in the seed mixture of the tray.

To ensure a reduction in separation time (increasing productivity), we accept the following hypothesis: the periodic change in the direction of rotation of the trier cylinder affects the quality and productivity of the separation process

The following factors were selected for the research: duration of cylinder rotation counterclockwise T_L (15, 25, 35 s) and clockwise T_R (1, 2, 3 s). The evaluation criteria are the number of seeds and impurity elements N_1 and the relative content of impurity elements ε_1 in the seed mixture of the tray. The numerical modeling was carried out according to a whole factorial experiment with a total number of experiments – $3^2 = 9$.

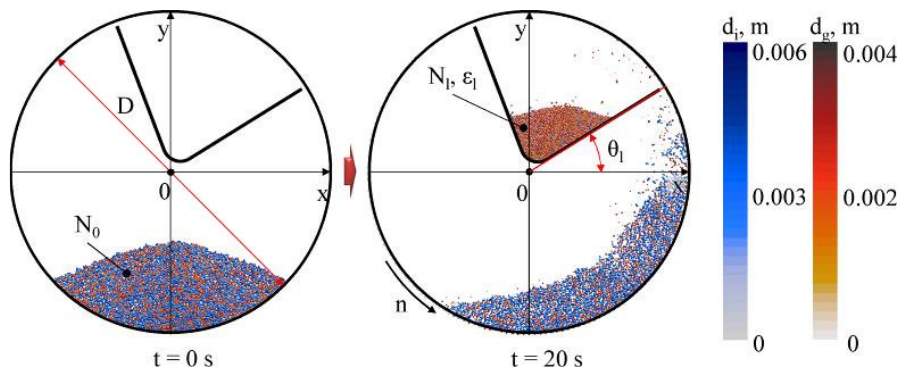


Fig. 8. Calculation scheme of a cylindrical cellules trier with a tray for numerical simulation in the STAR-CCM+ software package

After processing the data in the Wolfram Cloud software package, second-order regression equations need to be established to determine the dependence of the separation process criteria on the research factors. In the statistical processing of the data obtained in the Wolfram Cloud software package, each coefficient of the regression equation was analyzed using Student's criterion and compared with the table value. If the calculated value was less than the table value, the coefficient of the regression equation was insignificant and could be disregarded [20]. To check the adequacy of the obtained regression equation, the Fisher test and correlation coefficient were used [18].

3. Results

3.1. Simulation Results

Figures 9 to 11 depict the visualization obtained as a result of the numerical modeling of the process of separating the seed material of small-seeded crops using a cylindrical cellules trier.

The visualization presented in Figure 9 depicts the process of seed material separation of small-seeded crops on a cylindrical cellules trier, illustrating the

influence of the initial number of seeds and impurity elements in the seed mixture (N_0).

The figure shows three cross-sectional flat images of trier cylinders with a constant diameter $D = 0.4$ m, with a constant cylinder rotation frequency $n = 45$ rpm. In the first case, the number of seeds $N_0 = 1000$ pcs.; in the second case, $N_0 = 3000$ pcs. In the third case, $N_0 = 5000$ pcs. During the rotation of the cylinder, in each case, the seed material rises to a certain height along the trajectory of the cylinder. With the smallest number of seeds (at $N_0 = 1000$ pcs), the more significant part (25.3%) of the seed material rises in the direction of rotation of the cylinder from the starting point to the angle θ , at $N_0 = 3000$ pcs, a more significant amount of seed material rises - 32.2% of the total amount, with $N_0 = 5000$ pieces - even higher (36.6%). It can be seen from the figure that with an increase in the amount of seed material, a so-called "dead layer" of material is formed, which is indicated in the figures by white areas in the form of an arc. This region is called dead due to the lack of mixing of the layers of seed material since the constant frequency and diameter of the cylinder are not suitable for separating a large

amount of seed material. Removal of the «dead layer» with a more significant amount of seed material can be achieved

by increasing the trier cylinder's rotation frequency or the cylinder's diameter.

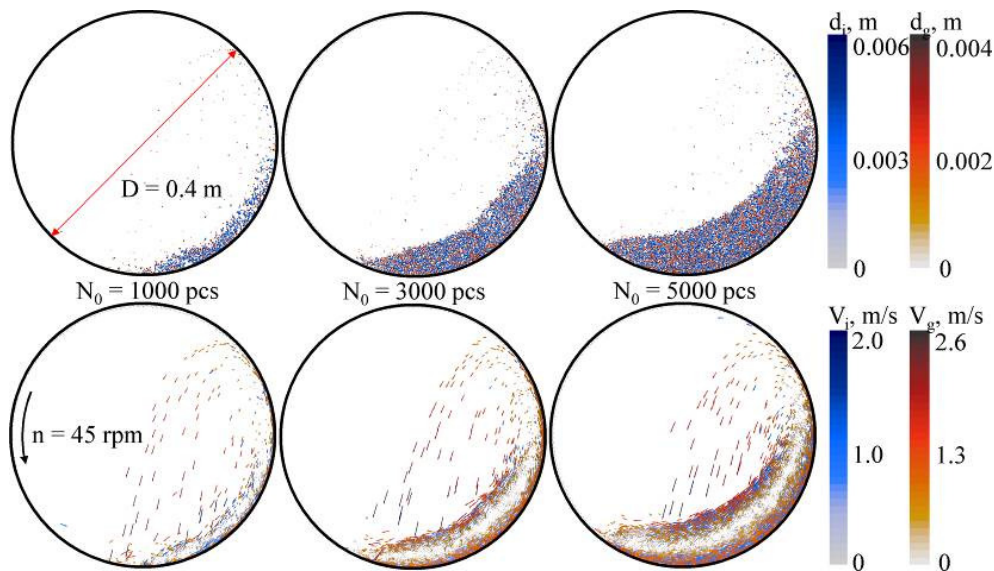


Fig. 9. Visualization of the process of separating seed material of small-seeded crops in a cylindrical cellules trier depending on the number of seeds and impurity elements in the seed mixture N_0

Figure 10 illustrates the visualization of the process of seed material separation for small-seeded crops using a cylindrical cellules trier, dependent on the rotation frequency of the trier cylinder n . The figure shows three cross-sectional flat images of trier cylinders with a constant diameter $D = 0.4$ m, a constant amount of seed material $N_0 = 3000$ pcs., and different rotation frequencies of the cylinders $n = 30$ rpm, $n = 45$ rpm, $n = 60$ rpm. In the case of the lowest rotation frequency $n = 30$ rpm, most of the seed material does not reach the regions θ_{\min} and θ_{\max} , which means that the selected frequency is

ineffective. Also, the figure shows a «dead layer» of seed material, the amount of which can be reduced by increasing the rotation frequency of the cylinder. At the cylinder rotation frequency $n = 45$ rpm, the seed material reaches the region of θ_{\min} and θ_{\max} , but in this case, a "dead layer" is also present. In the case of the cylinder rotation frequency $n = 60$ rpm, the seed material passes through the region θ_{\min} and θ_{\max} , but at the same time, the dead layer decreases. The most appropriate is the average rotation frequency of the cylinder, namely $n = 45$ rpm.

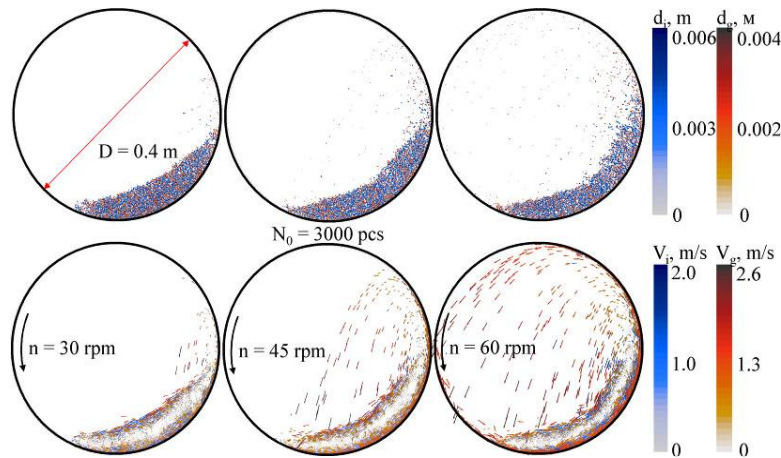


Fig. 10. Visualization of the process of separating seed material of small-seeded crops in a cylindrical cell trier depending on the rotation frequency of the trier cylinder n

Figure 11 depicts a visualization of the seed material separation process for small-seeded crops using a cylindrical seed

trier, with a variation in the diameter of the trier cylinder D .

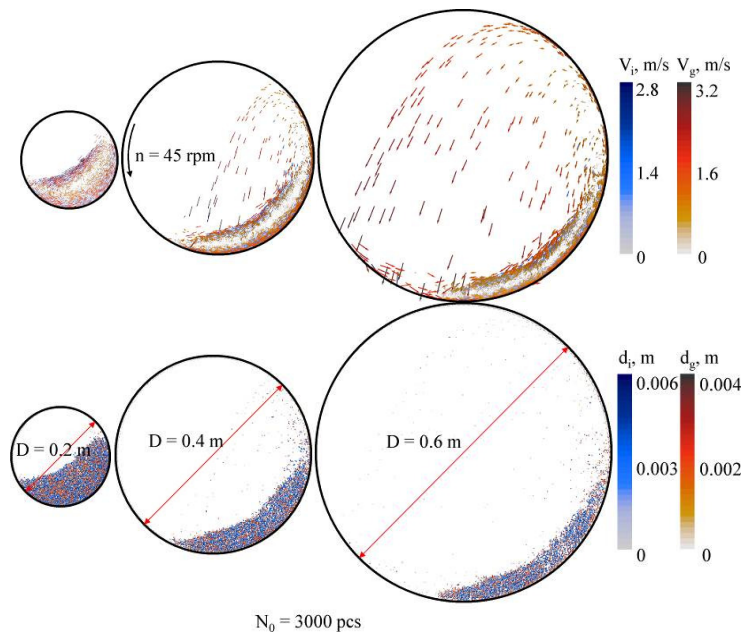


Fig. 11. Visualization of the process of separation of seed material of small-seeded crops in a cylindrical cell trier depending on the diameter of the trier cylinder D

The figure shows three flat images of the trier cylinders in a cross-section with a constant amount of seed material $N_0 = 3000$ pieces, a constant rotation

frequency $n = 45$ rpm min. and different diameters of the cylinder, which are $D = 0.2$ m, $D = 0.4$ m, $D = 0.6$ m. At the minor diameter of the cylinder, the seed

material fills the inner area almost half; when the cylinder rotates, only a tiny amount of seed material rises to the region between θ_{\max} and θ_{\min} , while the rest of the mass forms a «dead layer». Therefore, it is impractical to use the minor diameter of the cylinder in further studies since the separation efficiency, in this case, will be minimal.

In the case of the medium diameter, during the rotation of the cylinder, the seed material rises to the region between θ_{\min} and θ_{\max} . In the case with the largest diameter $D = 0.6$ m, during the rotation of the cylinder, most of the seed material passes the region between θ_{\min} and θ_{\max} . Still, it is in this case that the most thinnest «dead layer» is observed, unlike

in the first two cases. It can be seen from the figure that it is most expedient to use a cylinder with a diameter of $D = 0.4$ m in further research.

The data obtained was processed using the Wolfram Cloud software package to obtain a second-order regression equation, which reveals the relationship between the values of the minimum θ_{\min} and maximum θ_{\max} of the seed exit angles from the trier cylinder cellules and the research factors in a simplified form by eliminating the insignificant regression coefficients (Equations (3) and (4)).

Graphical interpretation of dependencies (3)–(4) is presented in Figure 12.

$$\theta_{\min} = -0.0858955 + 0.12522 \cdot D - 0.630707 \cdot D^2 + 0.00831824 \cdot n - 0.000124883 \cdot N_0 + 2.71427 \cdot 10^{-6} \cdot n \cdot N_0 + 9.1622 \cdot 10^{-9} \cdot N_0^2 \quad (3)$$

$$\theta_{\max} = -0.786462 + 1.43559 \cdot D - 1.84779 \cdot D^2 + 0.020566 \cdot n + 0.0317732 \cdot D \cdot n \quad (4)$$

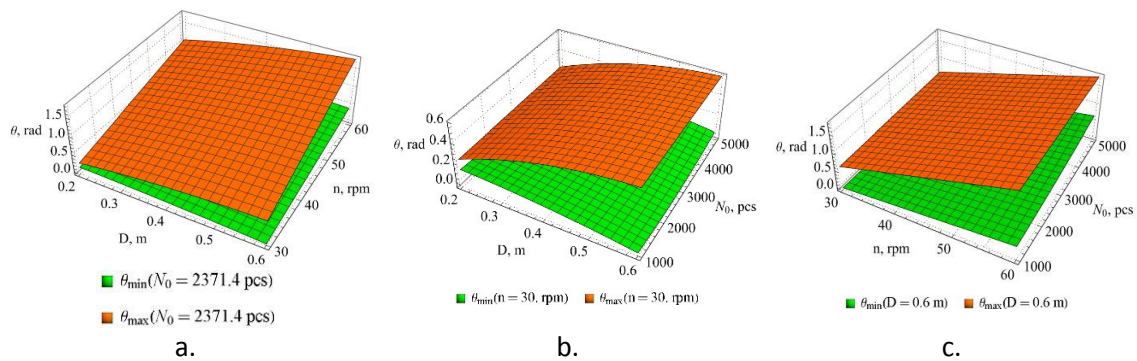


Fig. 12. The minimum ϑ_{\min} and maximum ϑ_{\max} values of the angles of seed exit from the cellules of the trier cylinder are dependent on the diameter of the trier cylinder D , the rotation frequency of the trier cylinder n , and the number of seeds and impurity elements in the seed mixture N_0

The statistical analysis conducted on equations (3) and (4) within the studied range of variation revealed a Pearson correlation coefficient of 0.82 and 0.85, respectively. Furthermore, Fisher's criterion for both equations was found to be $F(3) = 2.27 < F_t = 2.49$ and $F(4) = 2.17 < F_t = 2.49$, respectively. These results demonstrate the adequacy of the obtained models.

The data obtained was processed using the Wolfram Cloud software package to

$$N = 534.531 - 1,414.9 \cdot D + 1,193.5D^2 - 17.88 \cdot n + 19.7533 \cdot D \cdot n + 0.132741 \cdot n^2 + 0.03816 \cdot N_0 - 0.2215 \cdot D \cdot N_0 + 0.00302044 \cdot n \cdot N_0 \quad (5)$$

The optimal combination of factors for achieving the maximum amount of all components of the seed mixture ($N = 816$ pcs) is obtained when using $D = 0.2$ m, $n = 60$ rpm, and $N_0 = 5000$ pcs.

derive a second-order regression equation. This equation depicts the relationship between the number of components within the seed mixture N that fall within the minimum θ_{\min} and maximum θ_{\max} angles of rotation of the trier cylinder and the research factors, represented in a decoded form while disregarding insignificant regression coefficients:

Figure 13 illustrates the graphical representation of the relationship described in equation (5).

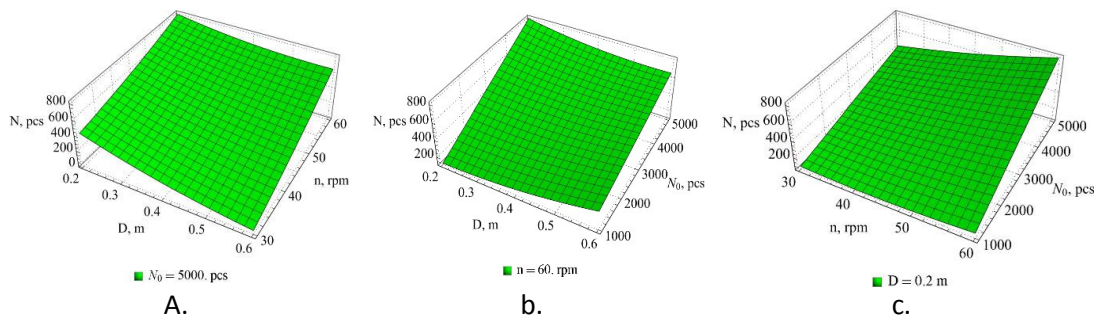


Fig. 13. The relationship between the number of all components of the seed mixture N that fell within the angles of rotation (ϑ_{\min} and ϑ_{\max}) of the trier cylinder and the diameter of the cylinder of the trier (D), the rotational speed of the cylinder of the trier (n), and the number of seeds and impurities in the seed mixture (N_0)

After the statistical analysis of equations (5) within the studied range of variation, it was found that the Pearson correlation coefficient is 0.83. Additionally, Fisher's criterion is $F(5) = 1.11$, which is less than the table value $F_t = 1.87$. This confirms that the obtained models are adequate.

By processing the data obtained, a second-order regression equation was obtained using the Wolfram Cloud software package. This equation shows the dependence of the relative content of impurity elements ϵ in the seed mixture, which is within the minimum θ_{\min} and the

maximum θ_{max} angles of rotation of the seed-separation trier cylinder. The regression equation is presented in a

$$\begin{aligned} \epsilon = & 44.321 - 161.241 \cdot D + 131.278 \cdot D^2 + 0,376244 \cdot n + 0.000644556 \cdot N_0 - \\ & 0.00009763 \cdot n \cdot N_0 + 1.03014 \cdot 10^{-6} \cdot N_0^2 \end{aligned} \quad (6)$$

Under the condition of a minimum relative content of impurities in the seed mixture ($\epsilon = 3.02\%$), the optimal values of the factors are $D = 0.6\text{ m}$, $n = 30\text{ rpm}$, and $N_0 = 1734\text{ pcs}$. Figure 14 presents the graphical representation of the dependence (6) which shows the relationship between the relative content of impurity elements ϵ in the seed mixture

decoded form with the deviation of insignificant regression coefficients:

and the research factors, with insignificant regression coefficients deviation.

Upon the statistical analysis of equations (6) within the studied range of variation, it was observed that the Pearson correlation coefficient was 0.88. Furthermore, Fisher's criterion for the model was $F(6) = 1.81$, which is less than the critical value $F_t = 2.49$. This confirms that the obtained models are adequate.

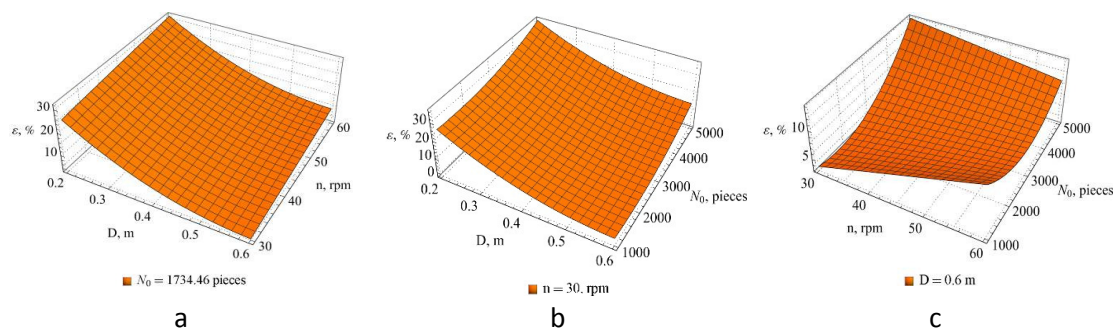


Fig. 14. The relative content of impurity elements ϵ in the seed mixture, which was within the minimum ϑ_{min} and maximum ϑ_{max} rotation angles of the cylindrical cellules trier cylinder, depends on the diameter of the trier cylinder D , the rotation frequency of the trier cylinder n , and the number of seeds and impurities in the seed mixture N_0

Because for each criterion of the evaluation of the experiment, the optimal values of the factors that do not coincide are determined, let's solve the compromise problem, which has the form:

$$\begin{aligned} \epsilon(D, n, N_0) & \rightarrow \min \\ N(D, n, N_0) & \rightarrow \max \end{aligned} \quad (7)$$

We will solve Problem (7) using the method of scalar ranking, where we minimize the multiplicative function by considering the importance coefficient of the individual criterion:

$$\frac{N}{\max(N)} / \frac{\epsilon}{\max(\epsilon)} \rightarrow \max \quad (8)$$

Upon solving Equations (8), (5), and (6) in the Wolfram Cloud software package, we derived rational structural and technological parameters for the trier separator: $D = 0.58$ m, $n = 46.8$ rpm, $N_0 = 2722$ pcs. With these parameters, the optimization criteria were as follows: $N = 251$ pcs., $\varepsilon = 5.89$ %, $\theta_{\min} = 0.22$ rad, and $\theta_{\max} = 1.26$ rad.

We will now examine the impact of changing the direction of the cylinder rotation on the separation process quality, using the parameters obtained above. Figure 15 shows a scalar and vector visualization of the process of separating small-seeded crop seed material using a cylindrical cellules trier with a tray.

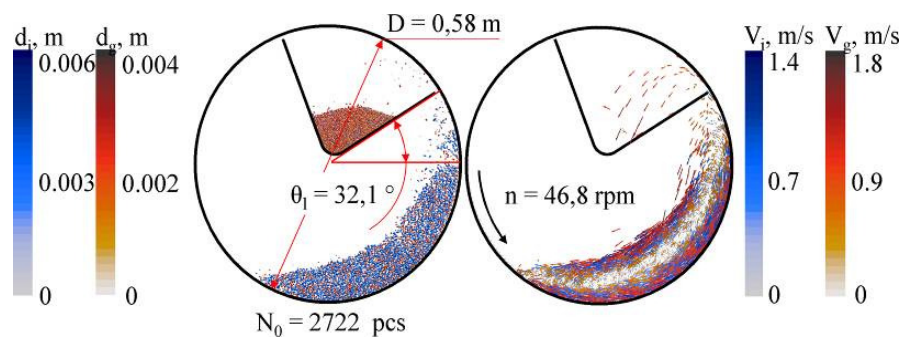


Fig. 15. *Scalar and vector visualization of the process of separation of seed material of small-seeded crops in a cylindrical cellules trier with a tray*

Figure 16 shows the dynamics of changes in the number of seeds and impurity elements N_i and the relative content of impurity elements ε_i in the seed mixture of the tray. The analysis of the obtained dependence shows that when the value of $N_i = 1902$ pcs is reached, the growth of the number of components in the tray's seed mixture practically stops, indicating the complete movement of seeds to the tray. A slight further increase in the number of components in the seed mixture of the tray occurs due to the ingress of impurities, which in turn leads to an increase in the content of impurities ε_i in

the seed mixture of the tray. The optimal value of the separation time is $t_{\text{opt}} = 24.8$ s – the time the seed mixture stays in the cylinder, during which the best quality of separation is achieved at the highest productivity (the content of impurity elements in the seed mixture of the tray $\varepsilon_i = 4.9$ %). The conditional productivity of the process is $Q_i = N_i/t_{\text{opt}} = 76.7$ pcs/s.

Figures 17 and 18 presents a visualization obtained through a numerical modeling of the separation process of seed material from small-seeded crops using a cylindrical cellules trier with variable rotation frequency.

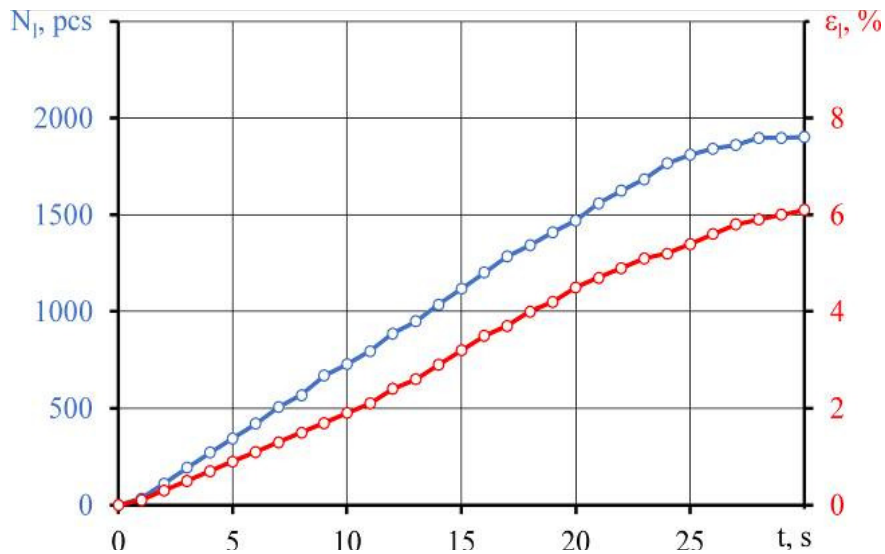


Fig. 16. The number of seeds and impurities (N_i) and the relative content of impurities (ε_i) in the seed mixture of the tray are subject to changing dynamics

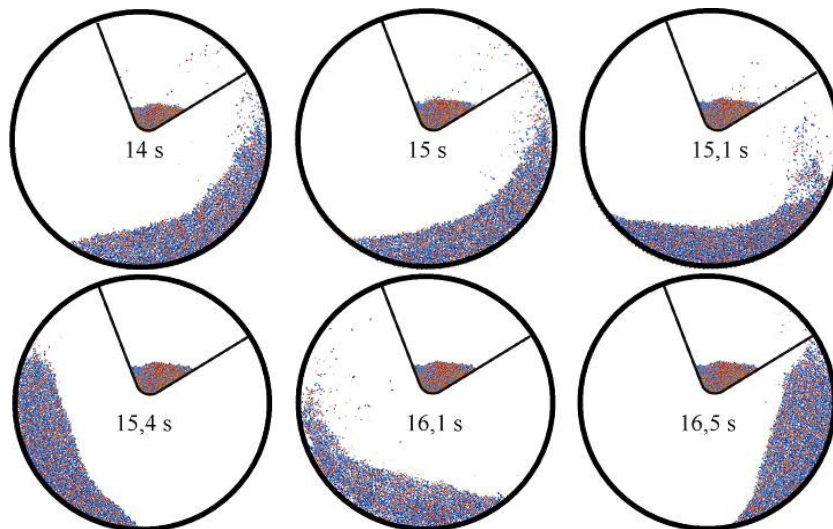


Fig. 17. The distribution of the components in the seed mixture can be visualized in a cylindrical cellules trier with variable cylinder rotation frequency at $T_L = 15$ and $T_R = 1$ s

By processing the data using the Wolfram Cloud software package, a regression equation was derived that expresses the relationship between the number of seeds and impurities (N_i) in the seed mixture of the tray and the research

factors in a decoded form, while taking into account the deviation of insignificant regression coefficients:

$$N_i = -1,568.7 + 224.8 \cdot T_L - 3.53778 \cdot N_L^2(9)$$

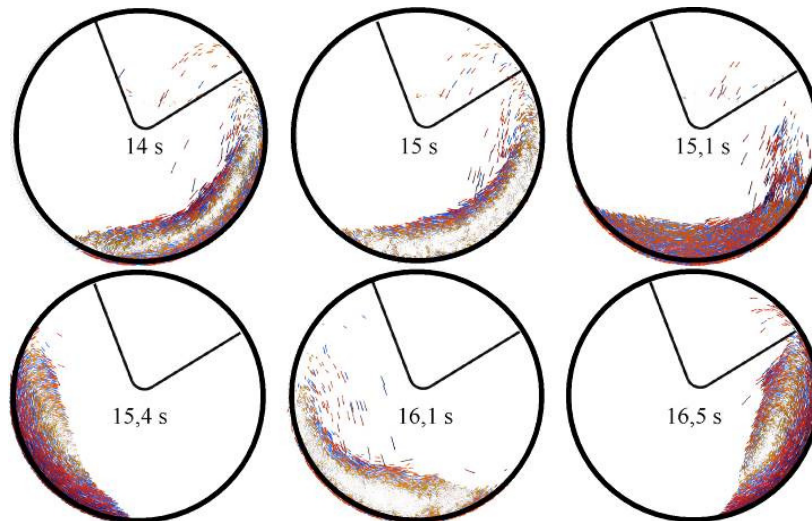


Fig. 18. The vector field of velocities of the components in the seed mixture can be visualized in a cylindrical cellules trier with variable cylinder rotation frequency at $T_L = 15$ s and $T_R = 1$ s

To achieve the maximum number of seeds and impurity elements in the seed mixture of the tray ($N_i = 2002$ pcs), the optimal values of the factors are $T_L = 31.7$ s and $T_R = 2$ s. A graphical representation of the relationship (9) can be found in Figure 19.

Upon the statistical analysis of Equations (9) in the studied variation range, it was found that the Pearson correlation coefficient is 0.90. Additionally, Fisher's criterion was calculated as $F(9) = 2.42$, which is less than the threshold value of $F_t = 2.93$. These results confirm the adequacy of the obtained models.

By processing the data using the Wolfram Cloud software package, a regression equation was derived that expresses the relationship between the relative content of impurity elements (ϵ_i) in the seed mixture of the tray and the

research factors in a decoded form, while taking into account the deviation of insignificant regression coefficients:

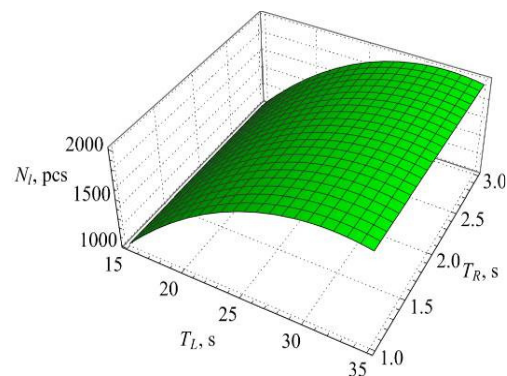


Fig. 19. The number of seeds and impurity elements (N_i) in the seed mixture of the tray is dependent on the duration of the counterclockwise (T_L) and clockwise (T_R) rotation of the cylinder

$$\epsilon_i = 5.26601 - 0.139206 \cdot T_L + 0.00534921 \cdot T_L^2 - 0.244444 \cdot T_R \quad (10)$$

To minimize the relative content of impurity elements in the seed mixture of the tray ($\epsilon_l = 3.64\%$), the optimal values of the factors are $T_L = 15$ s and $T_R = 3$ s. A graphical representation of the Equation (10) can be found in Figure 20.

Upon the statistical analysis of Equations (10) in the studied variation range, the Pearson correlation coefficient was found to be 0.87. Additionally, Fisher's criterion was calculated as $F(10) = 2.51$, which is less than the threshold value of $F_t = 2.93$. These results confirm the adequacy of the obtained models. Using the Wolfram Cloud software package, the obtained data was processed to obtain a regression equation that expresses the conditional dependence of the performance of the Q_N separator on the research factors in a

decoded form, while accounting for insignificant regression coefficients:

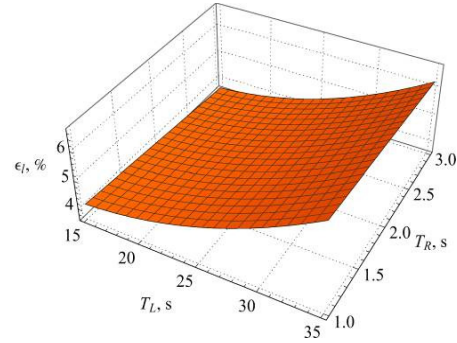


Fig. 20. *The relative content of impurity elements (ϵ_l) in the seed mixture of the tray depends on the duration of the counterclockwise (T_L) and clockwise (T_R) rotation of the cylinder*

$$Q_N = 7.54847 + 5.58074 \cdot T_L - 0.120338 \cdot T_L^2 - 3.91188 \cdot T_R + 0.0732822 \cdot T_L \cdot T_R \quad (11)$$

To achieve the maximum conditional productivity of the separator ($Q_N = 70.05$ pcs/s), the optimal values of the factors are $T_L = 23.5$ s and $T_R = 1$ s. A graphical representation of the Equation (11) can be found in Figure 21.

The statistical analysis of equations (11) within the studied variation range revealed that the Pearson correlation coefficient is 0.93, and Fisher's criterion is $F(11) = 2.23 < F_t = 2.93$. These results support the adequacy of the obtained models.

Because for each criterion of the evaluation of the experiment, the optimal values of the factors that do not coincide are determined, let's solve the compromise problem, which has the form:

$$\begin{aligned} \epsilon_l(T_L, T_R) &\rightarrow \min \\ Q_N(T_L, T_R) &\rightarrow \max \end{aligned} \quad (12)$$

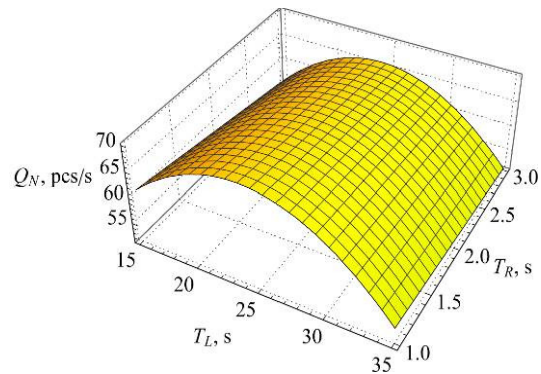


Fig. 21. *Dependence of the conditional productivity of the separator Q_N on the duration of rotation of the cylinder counterclockwise T_L and clockwise T_R*

The solution to problem (12) involves using the scalar ranking method, which minimizes the multiplicative function while considering the importance coefficient of the individual criterion:

$$\frac{Q_N}{\max(Q_N)} / \frac{\varepsilon_1}{\max(\varepsilon_1)} \rightarrow \max \quad (13)$$

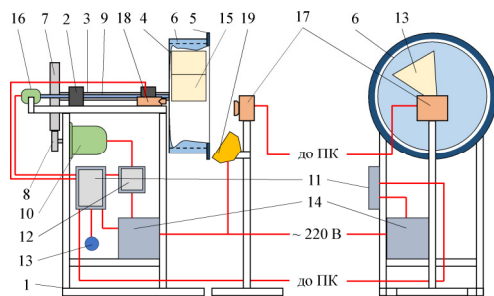
where *max* is the maximum value of the function.

The Wolfram Cloud software package was used to solve equations (13), (10), and (11) and obtain the rational mode parameters of the trier separator, which

are $TL = 20.8$ s and $TR = 1$ s. Using these parameters, the optimization criteria were $Q_N = 69.2$ pcs/s and $\varepsilon_1 = 4.44\%$.

3.2. Implementation of Results

A laboratory cylindrical cell trier was developed and created. The structural and technological scheme and the general view are shown in Figure 21. The working body is a cylinder, which consists of plates with shells. The plates are printed on an Anycubic S 3D printer from ABS+ plastic. The electrical control scheme is shown in Figure 22.



a.



b.

Fig. 21. Structural and technological scheme (a) and general view (b) of a laboratory cylindrical cell: 1 – bed frame; 2 – bearings; 3 – empty shaft; 4 – cylinder; 5 – glass cover; 6 – plates with cells; 7 – the pulley is known; 8 – drive pulley; 9 – solid shaft; 10 – direct current electric motor; 11 – Arduino UNO control board; 12 – L298N DC motor driver; 13 – potentiometer; 14 – power supply unit; 15 – tray; 16 – servo drive; 17 – video camera *Aspiring Repeat 4 Ultra HD 4K Dual Screen*; 18 – IR sensor; 19 – cold white lighting lamp (5000–6500K)

In the design of the laboratory cylindrical shell trier, it is possible to change the structural and operational parameters of the work process: replace plates with shells; change the cylinder rotation frequency – from 1 to 100 rpm; change the direction of rotation of the

cylinder; change the angle of rotation of the tray.

To change the rotation frequency of the cylinder and the direction of rotation, an Arduino UNO control board and a DC motor driver L298N were used (Figure 22). The frequency and direction of rotation of the cylinder can be controlled manually

using a potentiometer and automatically using the Arduino IDE monitor port. Control over the frequency of rotation of

the cylinder is carried out by an IR sensor, which is calibrated by a Benetech GM8906 contact tachometer.

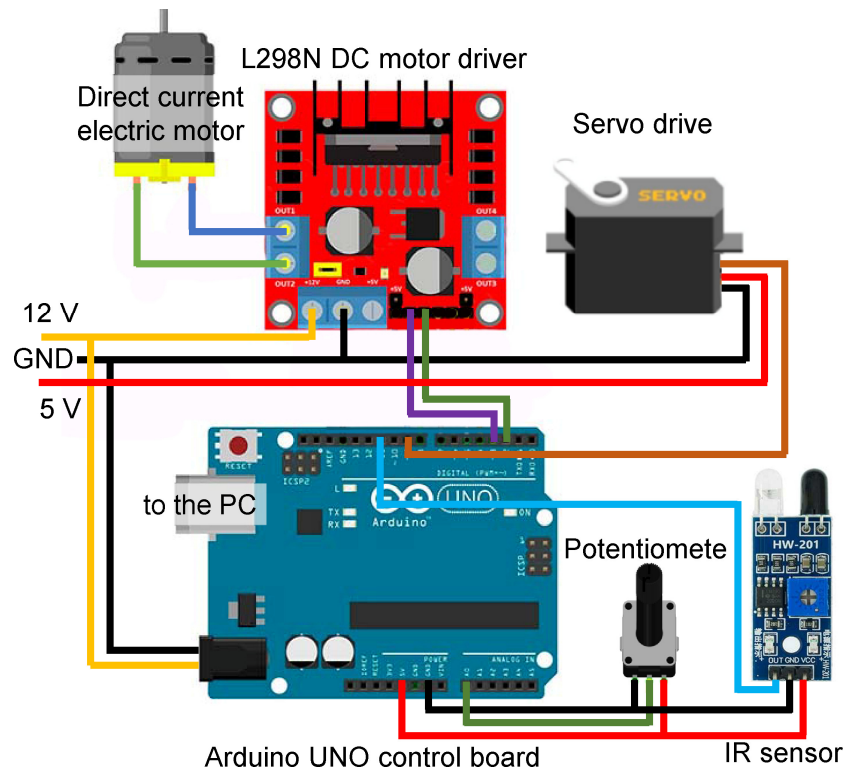


Fig. 22. *Electric control scheme of a laboratory cylindrical cell trier*

Plates with shells are fixed between themselves and the cylinder using connecting locks, which makes it impossible to accidentally shift the plates during the rotation of the cylinder. The tray can be quickly removed from the laboratory setup.

In order to assess the quality of the work of the cylindrical seed trier, the received video from the video camera must be visually analyzed and the trajectories of the seeds' movement during their flight in the cylinder must be calculated. This requires specialized software. As a result

of the information search, the basic program code of TracTrac, which was developed by Joris Heyman [12-14], was determined. The code is fully open source and written in the Python programming language using the OpenCV open source library. However, this software has been improved for our purposes.

As a result of the refinement of the code, the TracTrac software package made it possible to determine the trajectory of the flight and the speed of the seeds during their movement in the cylindrical cell trier (Figure 23).

Based on the received processed data of the video image, the frequency and direction of rotation of the cylinder and the angle of rotation of the tray are controlled.

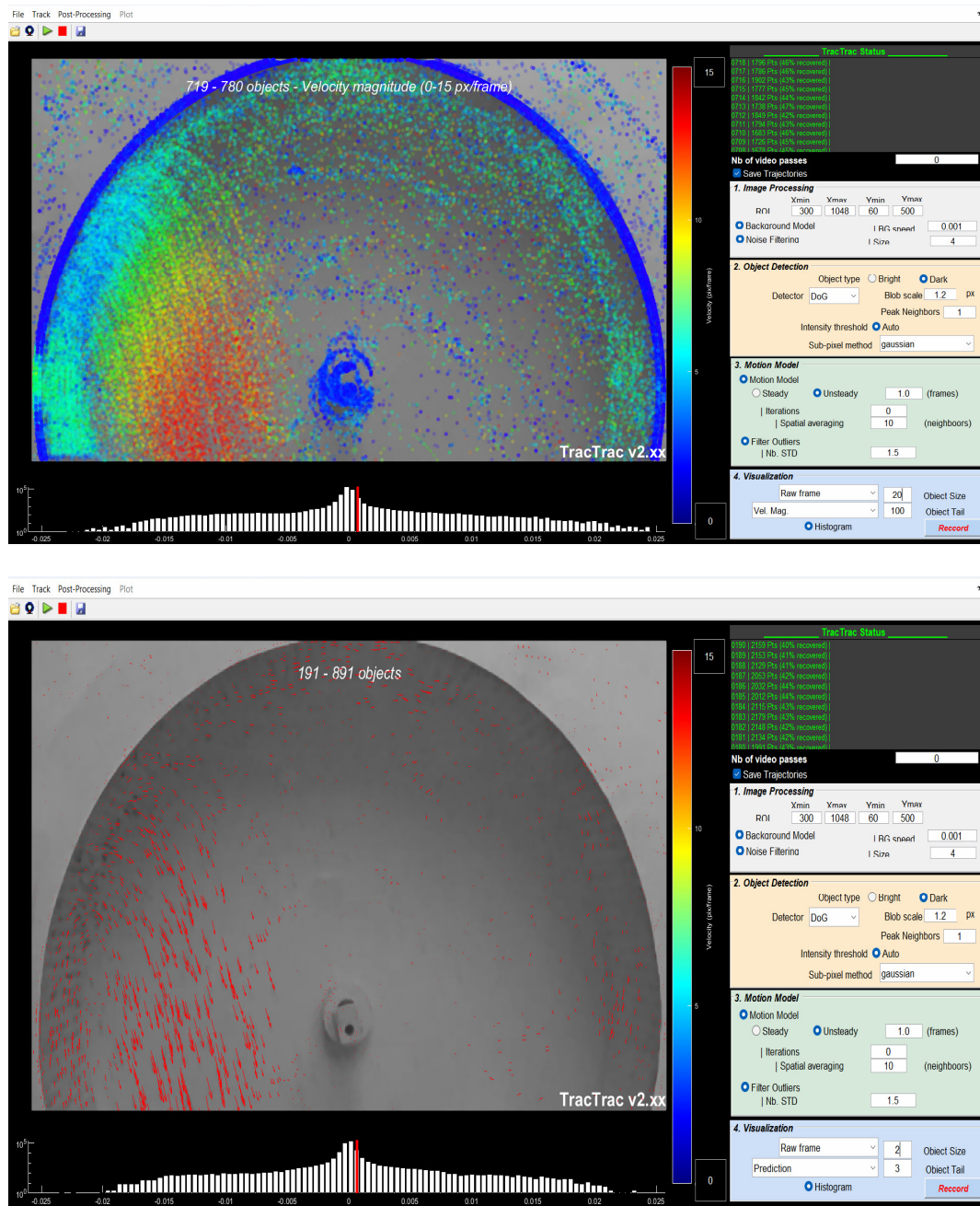


Fig. 23. Visualization of the advanced TracTrac software package to determine the speed of seeds during their movement in a cylindrical cell trier

4. Discussion

A model was developed in the Star CCM+ software package to simulate the process of separating seed material of small-seeded crops using a cylindrical seed-separation trier. Using mustard seeds as an example and considering initial and boundary conditions of the cylindrical trier, the visualization of the separation process was obtained with respect to the research factors, which were the number of seeds and impurity elements in the seed mixture (N_0), the rotation frequency of the trier cylinder (n), and the diameter of the trier cylinder (D).

The dependence of the minimum (θ_{\min}) and maximum (θ_{\max}) angles of seed exit from the trier cylinder cellules on the research factors was obtained in the form of second-order regression equations. The number of all components of the seed mixture (N) within these angles was taken as the performance criterion, and its dependence on research factors was also obtained as second-order regression equations.

The relative content of impurity elements (ϵ) in the seed mixture within the angles of rotation was chosen as the criterion for evaluating the quality of the separation process. The dependence of ϵ on research factors was also obtained in the form of second-order regression equations.

Additionally, the simulation results provided the dependence of the number of seeds and impurity elements (N_i) and the relative content of impurity elements (ϵ_i) in the seed mixture in the tray, as well as the conditional performance of the separator (Q_N), on the duration of cylinder rotation counterclockwise (T_L) and clockwise (T_R).

The Wolfram Cloud software package was used to solve the compromise problem by minimizing the multiplicative function that takes into account the importance coefficient of the private criterion using the scalar ranking method. The aim was to minimize the relative content of impurity elements ϵ and maximize the number of components of the seed mixture N that were within the minimum θ_{\min} and maximum θ_{\max} rotation angles of the cylindrical seed-separation trier. Based on this approach, the rational design and technological parameters of the cylindrical seed-separation trier were obtained. These parameters were $D = 0.58$ m, $n = 46.8$ rpm, and $N_0 = 2722$ pcs, and the optimization criteria achieved were $N = 251$ pcs, $\epsilon = 5.89\%$, $\theta_{\min} = 0.22$ rad, and $\theta_{\max} = 1.26$ rad.

After performing a numerical simulation of the process of separating small-seeded crop materials using a cylindrical seed drill at varying rotation frequencies, we obtained the dynamics of changes in the number of seeds and impurities N_i , as well as the relative content of impurity elements ϵ_i in the tray's seed mixture. The analysis of the obtained dependence reveals that once the value of N_i reaches 1902 pcs, the number of components in the tray's seed mixture practically stops growing, indicating that all seeds have moved to the tray. The optimal separation time is $t_{\text{opt}} = 24.8$ s, which is the time the seed mixture stays in the cylinder, during which we achieve the best separation quality and highest productivity (the content of impurities in the seed mixture of the tray $\epsilon_i = 4.9\%$). The process's conditional productivity is $Q_i = N_i/t_{\text{opt}} = 76.7$ pcs/s.

By minimizing the multiplicative function and considering the importance

coefficient of the private criterion in the Wolfram Cloud software package, we solve the compromise problem using the scalar ranking method. As a result, we obtain the rational mode parameters of the cylindrical seed-separation trier, which are $T_L = 20.8$ s and $T_R = 1$ s. With these parameters, the optimization criteria are $Q_N = 69.2$ pcs/s and $\varepsilon_1 = 4.44$ %.

Based on the obtained dependencies of the numerical modeling and the results of improvement of the TracTrac software package, a laboratory sample of an adaptive cylindrical cell trier was developed. This trier allows in real time, based on the received video image, to determine the trajectory of the seed flight and to control the position of the tray and the rotation frequency of the cylinder using Arduino UNO.

References

1. Aliiev E., Lupko K., 2021. Prerequisites for the creation of a mechatronic system of indented cylinders for the separation of fine seeds. In: *Scientific Horizons*, vol. 24(3), pp. 75-86.
2. Aliiev E.B., 2019. Physico-mathematical models of processes of precision separation of sunflower seed material. Monograph, STATUS Publishing House, Zaporizhzhia, Ukraine, 196 p.
3. Aliiev E.B., Bandura V.M., Pryshliak V.M. et al., 2018a. Modeling of mechanical and technological processes of the agricultural industry. In: *INMATEH – Agricultural Engineering*, vol. 54(1), pp. 95-104.
4. Aliiev E.B., Yaropud V.M., Dudin V.Yr. et al., 2018b. Research on sunflower seeds separation by airflow. In: *INMATEH – Agricultural Engineering*, vol. 56(3), pp. 119-128.
5. Bai C., 1996. Modelling of spray impingement processes. Ph.D Thesis, University of London, United Kingdom, 449 p.
6. Bakin I.A., Belousov G.N., Sablinsky A.I., 2001. Modeling of the mixing process by the entropy-information method. In: *New Technologies in Scientific Research in Education, Materials of the All-Russian Scientific-Practical Conference, Part 1*. Yurga, Russian Federation.
7. Brandenburg N., 1977. The principles and practice of seed cleaning: separation with equipment that senses dimension, shape, density, and terminal velocity of seeds. In: *Seed Science and Technology*, vol. 5, pp. 173-186.
8. Broas P., 2001. Advantages and problems of CAVE-visualisation for design purposes. In: *Trans – VTT Symposium Virtual Prototyping*. Espoo, February 1st, pp. 73-81.
9. Desai B., 2004. Drying, cleaning, and upgrading. In: *Seeds Handbook: Processing And Storage*, CRC Press, pp. 477-511.
10. Han S.W., Lee W.J., Lee S.J., 2012. Study on the particle removal efficiency of multi inner stage cyclone by CFD simulation. In: *World Academy of Science, Engineering and Technology*, vol. 6, pp. 411-415.
11. Harmond J., Brandenburg N., Jensen L., 1965. Physical properties of seed. In: *Transactions of ASAE*, vol. 8, pp. 30-32.
12. Heyman J., 2019. TracTrac: a massive object tracking algorithm to measure earth surface dynamics. In:

- Computers and Geosciences, vol. 128, pp. 11-18. DOI: [10.1016/j.cageo.2019.03.007](https://doi.org/10.1016/j.cageo.2019.03.007).
13. Heyman J., Girault G., Guevel Y. et al., 2013a. Computation of Hopf bifurcations coupling reduced order models and the Asymptotic Numerical Method. In: *Computers and Fluids*, vol. 76, pp. 73-85. DOI: [10.1016/j.compfluid.2013.02.001](https://doi.org/10.1016/j.compfluid.2013.02.001).
 14. Heyman J., Mettra F., Ma H.B. et al., 2013b. Statistics of bedload transport over steep slopes: Separation of time scales and collective motion. In: *Geophysical Research Letters*, vol. 40(1), pp. 128-133. DOI: [10.1029/2012GL054280](https://doi.org/10.1029/2012GL054280).
 15. Iguchi M., Ilegbusi O.J., 2014. *Basic transport phenomena in materials engineering*, Springer, 260 p.
 16. Ivanets V.N., Bakin I.A., Belousov G.N., 2002. Entropy approach to the evaluation of the process of mixing bulk materials. In: *Storage and Processing of Agricultural Raw Materials*, vol. 11, pp. 16-18.
 17. Jayas D., Cenkowski S., 2006. Grain property values and their measurement. *Handbook of Industrial Drying*, Edited by Mujumdar A., pp. 575-603.
 18. Kiselov O.V., Komarova I.B., Milko D.O. et al., 2022. Statistical processing and registration of the results of experimental studies (from the knowledge of the writing of dissertation studies). *Heading guide*, Institute of Mechanization of Production of the National Academy of Sciences, Electronic analogue of other research (electronic book: Zaporizhnaya), STATUS, 1599 p.
 19. Kubicki D., Lo S., 2012. Slurry transport in a pipeline – Comparison of CFD and DEM models. In: *9th International Conference on CFD in the Minerals and Process Industries*, CSIRO, pp. 1-6.
 20. Odintsov D.V., 2001. Improving the efficiency of functioning of a cylindrical trier with a polymeric cellular surface by substantiating the main parameters and modes of operation. *Dissertation Thesis*, Moscow, Russian Federation, 161 p.
 21. Saqr K.M., Aly H.S., Wahid M.A. et al., 2009. Numerical simulation of confined vortex flow using a modified k-e turbulence model. In: *CFD Letters*, vol. 1(2), pp. 87-94.
 22. Satish G., Kmar A.K., Prasad V.V. et al., 2013. Comparison of flow analysis of a sudden and gradual change of pipe diameter using fluent software. In: *IJRET: International Journal of Research in Engineering and Technology*, vol. 2, pp. 41-45.
 23. Shevchenko I., Aliiev E., 2018. Study of the process of calibration of confectionery sunflower seeds. In: *Food Science and Technology*, vol. 12(4), pp. 135-142. DOI: [10.15673/fst.v12i4.1209](https://doi.org/10.15673/fst.v12i4.1209).
 24. Shevchenko I., Aliiev E., 2020. Improving the efficiency of the process of continuous flow mixing of bulk components. In: *Eastern-European Journal of Enterprise Technologies*, vol. 6/1(108), pp. 6-13. DOI: [10.15587/1729-4061.2020.216409](https://doi.org/10.15587/1729-4061.2020.216409).
 25. Shevchenko I., Aliiev E., Viselga G. et al., 2021. Modeling separation process for sunflower seed mixture on vibro-pneumatic separators. In:

- Mechanika, vol. 27(4), pp. 311-320.
DOI: 10.5755/j02.mech.27647.
26. Wallin S., 2000. Engineering turbulence modeling for CFD with a focus on explicit algebraic Reynolds stress models. PhD Thesis, Norstedts Truckeri, Stockholm, Sweden, 124 p.
27. Zaika P., 2006. Theory of agricultural machinery. Seed Cleaning and Sorting, Oko Publishing House, Kharkiv, Ukraine, 407 p.